Structuring with anisotropic colloids

Unilever R&D

Structuring with anisotropic colloids

Marjolein Dijkstra [1], Antina Ghosh [2], Jens Harting[4], Martin van Hecke[5], Alexander Siemens[5], Badr Kaoui[4], Vinzenz Koning[5], Karol M. Langner[5], Irene Niessen[6], José Francisco Paredes Rojas[2], Simeon Stoyanov[3]

[1] *University Utrecht, the Netherlands*
[2] *University of Amsterdam, the Netherlands*
[3] *Unilever, the Netherlands*
[4] *Eindhoven University of Technology, the Netherlands*
[5] *Leiden University, the Netherlands*
[6] *Radboud University Nijmegen, the Netherlands*

1. Abstract

Structure is an important factor in food. One of the ways to provide structure to foods is by using bubbles and foams. However, they need to be stabilized. One way of doing this is by covering them with microscopic rods. These rods self-assemble at the surface, yielding a stable bubble. The goal of this work is to gain a better understanding into how this self-assembly works using analytical calculations, experiments and simulations.

2. Company profile

Unilever is one of the world's leading fast-moving consumer goods companies. Our foods, home and personal care products are sold in over 180 countries and used by more than 2 billion consumers every day. Unilever is world leader in several consumer goods categories like savoury, dressings, tea, ice cream, spreads and deodorants. In 2010 Unilever employed over 167,000 people and was operating in 180 countries with a turnover of € 44.3 Billion, and had more than 12 global brands with sales of more than € 1 billion. Around € 6 billion were invested in advertising and promotion and € 928 million in R&D. Unilever files more than 300 new patent applications each year and has a portfolio of more than 20,000 patents and patent applications. Unilever R&D employs more than 6,000 professional researchers, working in 6 strategic R&D laboratories delivering groundbreaking technologies, 31 major development centres developing and implementing product innovations and 92 locations around the globe with R&D teams implementing innovations in countries and factories.

3. Problem description

From a physical-chemical point of view Unilever products are hierarchically structured multi-component colloidal liquids, semi/soft solids or solids that have certain desired behaviour upon production, storage and in-use. Some of these products are water continuous (like mayonnaise, sauces, ice-cream, conditioners) and some are oil continuous (like margarines, cheese, some skin-creams or deo–sticks). Therefore it is critical to have a set of

bulk structuring technologies that can deliver consumer benefits in a cost- and energy efficient way, utilizing sustainable raw materials and processes. In many cases (bio)polymers are used to structure bulk phases, but in some cases particles or droplets are used as well. It is well known that shape-anisotropic colloids are more efficient space fillers, thus they can provide similar structuring with less material as compared to spherical analogs. The structuring efficiency of these systems depends on colloid volume fraction, aspect ratio, size, polydispersity, flexibility/rigidity as well as particle-particle, particle-solvent and particle-other colloids interactions. There is a large body of theoretical and modelling studies in the open literature that predict the rheo-mechanical behaviour of anisotropic colloidal systems at a qualitative level, or in very specific cases quantitatively. However, what is still missing is a comprehensive approach, allowing to predict the behaviour of one and the same system for a broad range of concentrations, particle polydispersities and aspect ratios, especially for interacting systems, taking into account local solvent hydrodynamics or elasto-mechanics around the particles.

One of the techniques found by Unilever to add more structure to materials is by using air. A liquid can appear to be more solid if it contains bubbles. Unfortunately, such a foam will in general collapse over time, so for a consumer product the bubbles have to be stabilized. One way of doing this is by adding $CaCO_3$ rods to the material. These rods attach to the surface of the bubbles and stabilize them. Although this works in practice for a number of known formulations, it is not yet understood why the rods arrange themselves on the surface of the bubbles the way they do.

4. Problem solving strategy

Our goal is to gain a better understanding of the self-assembly of rods on curved surfaces.

In order to tackle this problem, we take four approaches, which we will discuss in more detail in the following sections. First we will discuss the knowledge that exists in the literature about self-assembly of rods and other objects on curved or flat surfaces.

When covering a surface, the covering particles in general will tend to align, but on curved surfaces the particles cannot be completely ordered. Therefore defects will be generated. We will investigate these defects analytically in section 6.

The bubbles under consideration are microscopic objects. However, the characteristic ordering of the rods is predominantly a geometric effect and therefore it might be possible to reproduce the covering in a macroscopic setting. This would facilitate further research. We present some experiments into this area in section 7.

It seems that currently the most comprehensive way to describe the self-assembly of the rods and other anisotropic particles is using simulations. We will present two simulations based on different methods in section 8.

5. Literature search

The phase behavior, alignment and structure of an assembly of anisotropic colloidal particles are long standing scientific issues, which have been studied in the past using computer simulations, theory and experiments. One of the earliest theoretical calculations for a three dimensional gas of infinitely thin hard rods is by Onsager in 1949 [1] where he had considered the orientational as well as the translational component of entropy and predicted an istotropic-nematic phase transition as the density of rods increases. Since then, many studies have been aimed at understanding and determining the structure and ordering of systems composed of ellipsoidal [2] and spherocylindrical particles [3] as a function of their shape anisometry.

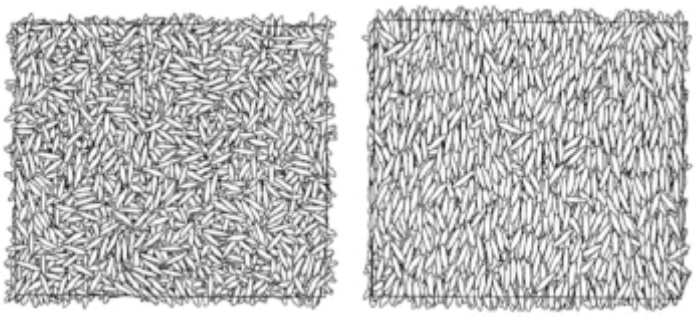

Figure 1. Phase transition of a system of hard rigid rods on a 2D flat surface. Left figure shows istotropic phase at lower densities. Nematic phase with orientational order is observed at higher densities as shown on the right panel (see [1] for details).

Geometry and structure of these particles on two dimensional surfaces is another important issue that has drawn much interest such as in depletion layers outside a spherical surface, drug capsules, viral capsids where structured surfaces are generated by the self assembly of such particles on planar or curved surfaces. A significant part of research is thus motivated towards understanding the two dimensional ordering of anisotropic particles. In particular, we focus here on the thin rod like particles used for the stabilization of air bubbles in emulsions as described above. One of the first computer simulations that have studied the phase behavior of thin rodlike particles on 2D flat surfaces was performed by Bates et al. [4], involving rigid rods of various aspect ratios. Their results show the existence of an isotropic nematic phase transition for very long rods, whereas shorter rods exhibit an isotropic fluid–solid transition with increasing density. Other than the aspect ratio, rod size polydispersity is another factor that can sufficiently influence the ordering of rigid rods. This has been demonstrated by Monte Carlo in a related scenario, namely of thin hard platelets with a polydispersity in the diameter [5]. Particle size segregation is observed in two coexisting phases – *isotropic-nematic* – with larger particles tending to be found in the nematic phase.

Although literature exists that investigates structuring over planar surfaces, extension of such studies to curved surfaces remain fairly limited. Problems related to the optimal ordering of particles on curved surfaces begins with the century old Thomson problem of finding the minimum energy configuration of N particles on a sphere interacting by the Coulomb potential [6].

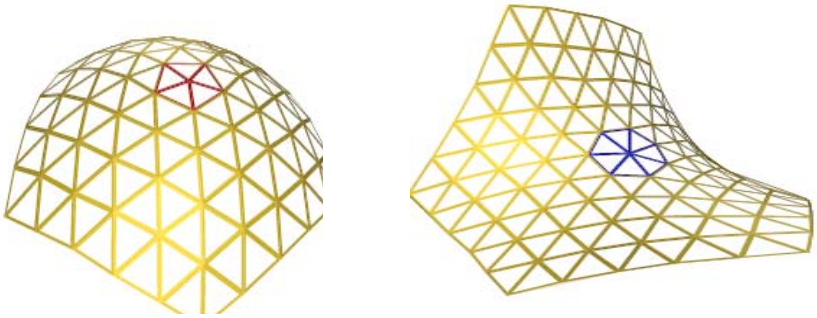

Figure 2. (Color lines) Examples of 5-fold (left) and 7-fold (right) disclinations on a triangular lattice in regions of positive and negative Gaussian curvature respectively (see [10] for details).

Analytical approaches to this problem are broadly based on expressing the elastic free energy as a function of curvature and number density, and subsequently minimizing it to determine the number of defects or grain boundaries [7-8]. In particular, in [7] the phase field crystal model is applied to study particle arrangement and dislocations on spherical surfaces

and derives scaling laws expressing the excess number of defects as a function of system size. Another study that deals with the ordering of hard spherocylinders on spherical droplets with computer simulations is reported in [9]. The simulation therein demonstrates the existence of isolated defects on curved surfaces, as well as density oscillations in their vicinity and the effective interactions between such defects. A recent review by Bowick et al. [10] provides a more general discussion about the two dimensional arrangement of particles on curved surfaces, related concepts and possible analytical treatment.

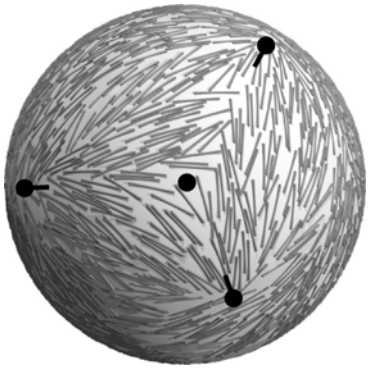

Figure 3. A triangular configuration of three positive defects around negatively charged defects (see [9] for details).

There have also been some interesting experimental observations recently of defects in relation to curvature [11-14]. An experimental report of the defect lines in spherical crystals has been published by Irvine et al. [11], where the experimental system is based on the self assembly of micron-sized polystyrene beads on water droplets and imaged with a phase contrast inverted microscope. In this study, the authors focused on detecting excess defects as a function of system size (radius of the sphere) and report the proliferation of excess defects beyond a critical size of the sphere.

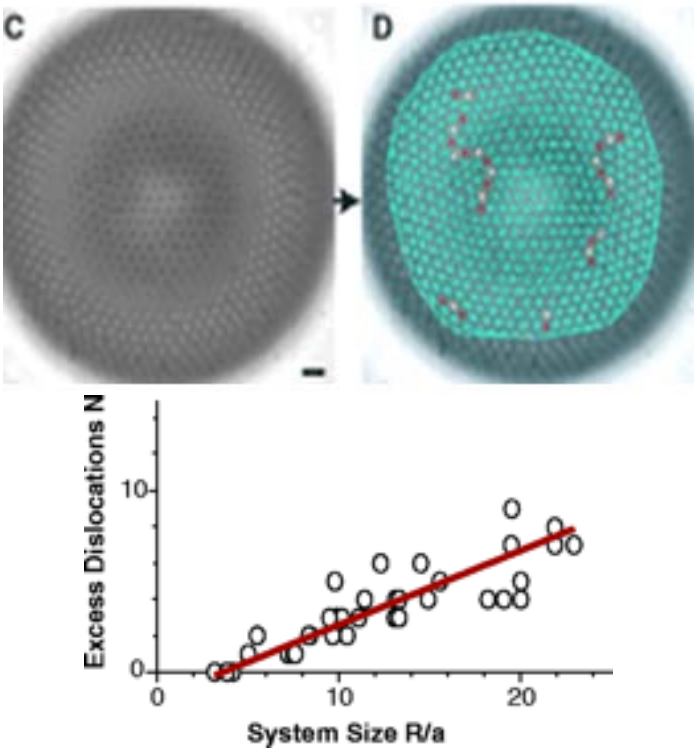

Figure 4. Top: Light microscope image of a particle coated droplet. Disclinations (defects) are shown in red or yellow respectively. Bottom: Number of excess dislocations

denoted by circles as a function of radius of the sphere, with the linear prediction given by the theory shown by the solid line.

Other available literature that presents detailed experimental studies and analysis to understand the properties of defects, geometric frustrations in curved surfaces and their local interactions with the curvature are reported in references [12-14].

In conclusion, there have been reports of the geometry and structures of beads and spherical particles on curved surfaces, although similar studies with rigid rods or anisotropic particles appear to be limited – thus presenting a scope for novel experiments or simulations to gain new insight.

6. Analytical calculations

In this section we investigate the role of curvature on an orientationally ordered phase. Details of this investigation can be found in references [15-18]. This analysis holds when spatial deformations of the orientation of the rods are small on the length scale of the rod, *L*, i.e. the bubble radius is orders of magnitude larger than *L*.

6.1 Elastic free energy

We construct a phenomenological free energy by punishing a spatial deformation of the local average orientation of the rods, ***n*** [19]:

$$F_{el} = \frac{1}{2} K \int d^2x \sqrt{g} D_\alpha n^\beta D^\alpha n_\beta$$

where the curvature is taken into account by including the determinant of the metric, *g*, and the covariant derivative, D^α, and *K* is an elastic constant. It is now possible to show that there must always be a misalignment if there is a non-vanishing Gaussian curvature [20]. Of course, this is the case for a spherical surface, where $S=1/R^2$. One can even rewrite the free energy entirely depending on defects (points where no preferred alignment can be determined) and curvature, instead of the average orientation of the rods:

$$F = \frac{K}{2} \int dA \int dA' \left(\rho\left(\mathbf{x}\right) - S\left(\mathbf{x}\right)\right) G_L\left(\mathbf{x}, \mathbf{x}'\right) \left(\rho\left(\mathbf{x}'\right) - S\left(\mathbf{x}'\right)\right)$$

From this expression it is possible to infer that defects are attracted to like-sign Gaussian curvature. Or put the other way around, if the surface is allowed to deform, ordered regions will flatten out the surface while defects curve the surface (e.g. positively charged defects will create cone-like surfaces). The free energy of a nematic ordered phase on the surface of a sphere has been calculated and is proportional to the number of defects:

$$F \propto N \log\left(\frac{R}{a}\right)$$

Furthermore, it was found both theoretically [15-17] and experimentally [18] that the ground state configuration has 4 defects of charge one half located on the vertices on the tetrahedron.

6.2 Success and breakdown

As can been seen from Figure 5 of a relatively large bubble, the rods are developing some orientational order. We can also identify defects in this ordered system. Two of them (of charge one half) have been indicated with red dots. This being said, very often these rigid

rods do not support a nematic phase, but rather a disordered domain phase. This lack of order is common for hard rods [19].

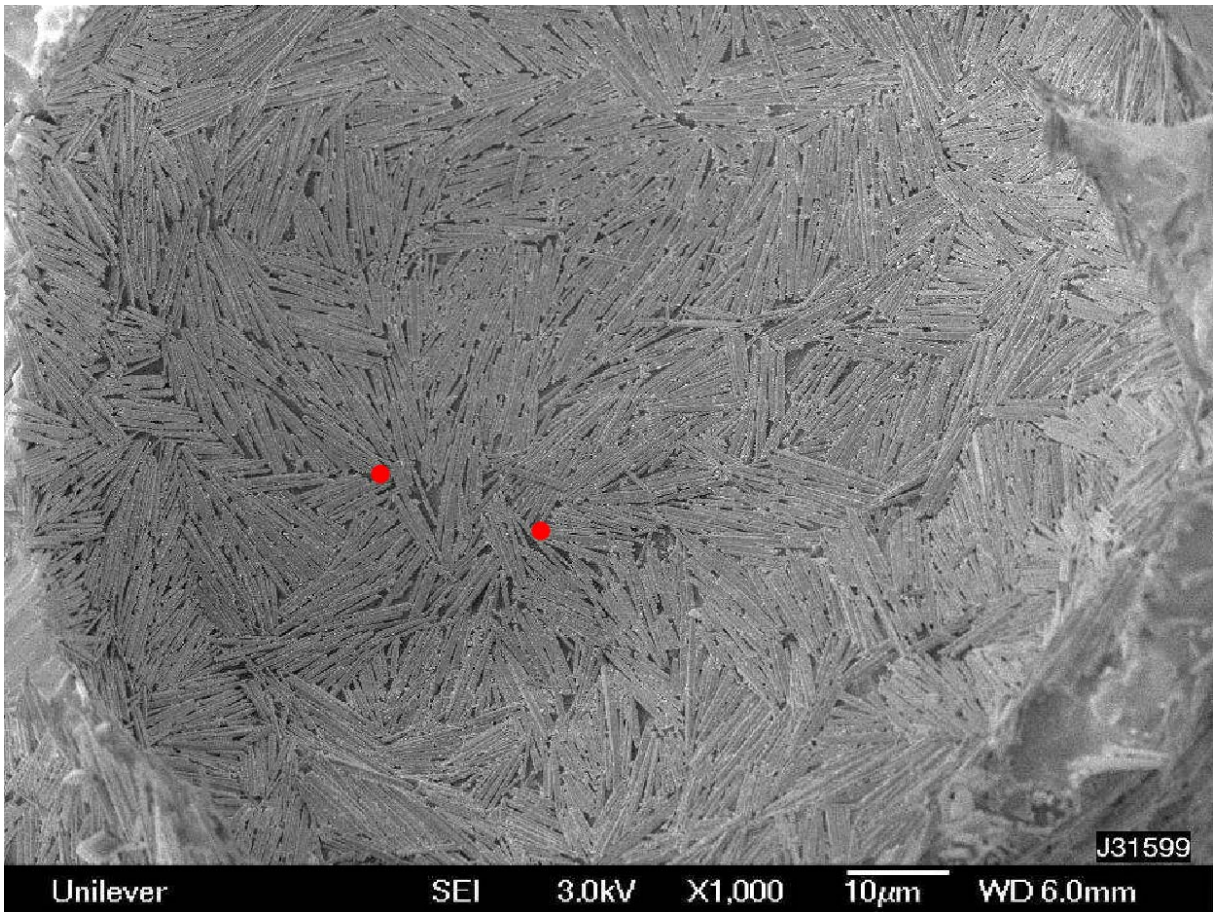

Figure 5. Image of a relatively large bubble on which rods are assembled. Orientational order seems to be developing in some regions. Two of the defects have been indicated by red dots.

6.3 Topological analysis of domains

Since generally the rods assemble into domains rather than forming a nematic phase, we will try a different approach. We observe that the domains typically are squares of size *L* by *L*. However, tiling a sphere with squares is impossible according to Euler's formula,

$$F - E + V = \chi$$

Here, F are the number of faces, E are the number of edges and V the number of vertices of the polyhedron. The Euler number χ=2 for a convex surface such as a sphere. From this equation one can deduce that one needs to incorporate a total of eight triangles to tile the sphere completely, as is shown in Fig6.

Figure 6. Cuboctahedron containing eight triangles. The number of squares is not fixed (Image taken from [20]).

Now it is possible to approximate how many squares, Q, and triangles, T, there must be on a spherical surface with area $S = 4 Pi R^2$, namely:

$Q = 4 \pi R^2 / L^2 - 4$

$T = 8$

leading to a total number of faces of

$F = 4 \pi R^2 / L^2 + 4$

Furthermore, it is possible to calculate the total length of the domain walls, Y, which is the number of edges times L:

$Y = 8 \pi R^2 / L - 4 L$

If we now introduce an energy cost for surface tension proportional to R^2 and a cost for the total length of the domain walls (i.e edges) with a prefactor that is proportional to the angle (proportional to L/R) that the faces make at the edges, we find there is a preferred value for the radius of the bubble which scales with the rod length to the power 2/3. This should be experimentally testable by using different sizes of the rods.

This crude model can be extended to include rectangular rather than square shaped faces. Moreover, it would be interesting to study the effect of polydispersity in the rod length.

7. Experiments

We performed two experiments to provide a quick and basic insight into the problem of packing hard rods onto a curved surface. The aim of the experiments is to observe on a macroscopic scale domain creation of the "rods" for varying curvatures. Rods consist of wooden matchsticks (aspect ratio 2mm x 550mm) and toothpicks (aspect ratio 2mm x 650mm).

A first set of experiments were carried out by rotating a table top driven by a stepper motor with a rotation rate, which could be set manually. By filling the bucket with tap water we created the so-called Newton bucket: at rest the water surface is flat. When increasing the rotation rate, the water creeps up the wall and creates a parabolic shape. By varying the rate we could thus create different "curvatures" of the water. The varying curvatures mimicked the different air bubble sizes presented in the original problem posed by Unilever. The next step involved adding wooden toothpicks or match sticks (with the head cut off to avoid the uneven weight distribution) to the water before the rotation was initiated. In either case we would vary the rotation speed and use a Canon camera with a high shutter speed to record how the toothpicks/matches aligned themselves along the curved water surface.

A second set of experiments consisted of coating the outside of a blown-up balloon with grease and attaching the toothpicks to the surface and then letting the balloon deflate. Photos were taken to record how the toothpicks rearranged on the surface during the deflating. Two initial configurations were used: either the toothpicks were put on in a pre-aligned configuration or they were attached in a random configuration.

7.1 Experiments with rotating table

The first experiment consisted of matches placed on the water surface, which were initially not arranged before a run was started and thus were in a random configuration before rota-

tion. Figure 7. shows photos of the bucket rotating matches in following the sequence: at the highest rotation speed, at intermediate speed and after stopping the rotation.

The second experiment consisted of toothpicks in the bucket on the water. Toothpicks were manually arranged before rotation in order to create a dense packing. Figure 8. shows photos of the rotating toothpicks before rotation, during rotation and after stopping rotation.

Results of the experiments depicted in Figure 7 and Figure 8 suggest that at slower rotation rates, i.e. lower curvatures; created domains are larger in width, which implies that there are more rods per domain.

(a) (b) (c)

Figure 7. Bucket rotating matches in water at: (a) at highest speed (~18 rad/s), (b) intermediate speed and (s) after rotation stops. At intermediate speed the creation of domains starts becoming visible and after cessation of rotation it is clear that rods create domains.

(a) (b) (c)

Figure 8. Bucket rotating toothpicks in water: (a) before rotation and manually packed rods, (b) at the highest rotation (~18 rad/s) and (c) after rotation stops. Due to rotation the manually packed configuration is destroyed. Conversely when rotation is decreased domains start to form.

7.2 Experiments with balloons

In the first experiment an inflated balloon coated with grease as a sticky agent was covered with toothpicks in a pre-arranged configuration. Figure 9. shows how the initially arranged toothpicks order themselves once the balloon was deflated. Because of the high elasticity of the balloon, when it was deflated the rods started having less contact with the surface until there was only a very small part touching the balloon, which meant that this experiment does not represent the microscopic behavior we aim to study. Nevertheless, toothpicks seemed to order while they were getting closer to one another while the balloon was deflating.

Even if this experiment was not the most suited to study the ordering of rods on a curved surface, we decided to carry out a second experiment starting with disordered toothpicks. In this second experiment we also observed that the toothpicks seemed to arrange themselves into domains while the balloon was deflating, as shown in Figure 10.

(a) (b) (c)

Figure 9. Inflated balloon coated with pre-arranged toothpicks: (a) initial, ordered configuration of the toothpicks on the balloon, (b) the jamming together of the toothpicks on the surface and (c) the final, deflated balloon with the toothpicks in apparent domain-like structure.

(a) (b) (c)

Figure 10. Inflated balloon coated with disorder toothpicks: (a) initial disorder coverage of toothpicks, (b) the jamming together of the toothpicks on the surface and (c) deflated balloon with apparent small domains.

7.3 Conclusions and Recommendations

Results presented in Figures 7. and 8. and images previously obtained at microscopic scale suggest that the formation of domains at the liquid-air interface is due to geometrical effects. Additionally, these experiments confirm that if rod-like particles are located at a liquid-air interface and are under the influence of small perturbations, they will tend to an organized state formed by domains of parallel particles. Furthermore, we observed that the domain-like structures formed on curved surfaces (rotating bucket with water) as well as in flat surfaces (stationary bucket after rotation).

It is worth noting that the formation of domains on flat and curved water surfaces is equivalent to the formation of domains in big microscopic bubbles, which is justified since the length of the matches/toothpicks is smaller than the radius of curvature of the water-in-bucket system.

We recommend to carry out further experiments using rod-like particles with different aspect ratios in order to study the influence of this parameter on the formation of domain-like structures in liquid-air interfaces.

8. Numerical Simulations

Computer simulations are proving to be promising in understanding the dynamic properties of particle-stabilized multiphase flows. However, the shortcomings of traditional simulation methods quickly become obvious: a suitable simulation algorithm is not only required to deal with simple fluid dynamics but has to be able to simulate several fluid species while also considering the structure and motion of particles as well as fluid-particle interactions. In fact, recently a number of new ideas have been introduced in order to unify granular and liquid descriptions, or to treat particles and liquids within a single theoretical/simulation framework. Some of these involve modified lattice Boltzmann (LB) methods [21-23] and field theoretic ideas merged with particle dynamics [24-26]. During this workshop, beside a hybrid LB/MD approach, a fully particle-based approach has been applied using Dissipative Particle Dynamics with rigid colloids representing the rods. The particles and their interactions are generally described by molecular dynamics or Langevin dynamics and both algorithms are coupled to correctly exchange momentum between the solid and the fluid phases of the suspension.

The lattice Boltzmann method can be seen as an alternative to conventional Navier-Stokes solvers and is well established in the literature. It is attractive for the current application since a number of multiphase and multicomponent models exist which are comparably straightforward to implement. The lattice Boltzmann method can be seen as a discretized form of the Boltzmann equation describing the dynamics of a fictitious ensemble of particles. Their motion and interactions are restricted to a regular lattice in space and time. In the limit of small Mach and Knudsen numbers it can be shown that the method recovers the Navier Stokes equations. It has become a very successful tool for modeling fluids in science and engineering. Compared to traditional Navier-Stokes solvers, it allows an easy implementation of complex boundary conditions and - due to the high degree of locality of the algorithm - is well suited for the implementation on parallel supercomputers.

A few groups have combined multiphase lattice Boltzmann solvers with known algorithms for suspended particles. Here, we follow an alternative approach based on the multicomponent lattice Boltzmann model of Shan and Chen which allows the simulation of multiple fluid components with surface tension. Our model generally allows arbitrary movements and rotations of rigid particles of arbitrary shape. Further, it allows an arbitrary choice of the particle wettability – one of the most important parameters for the dynamics of multiphase suspensions. For a detailed introduction to the method see Refs. 22 and 23, where our model has been applied to spherical and ellipsoidal particles at fluid interfaces. We have presented a thorough validation of the method for single particle situations and show that a transition from a so-called bijel to a Pickering emulsion can be found by varying the particle concentration, the particle's contact angle, or the volume ratio of the solvents. Further, we investigated the temporal evolution of the droplet/domain growth in emerging Pickering emulsions and bijels.

The particle description in the hybrid LB/MD approach used here follows a standard molecular dynamics algorithm where the dynamics is computed by following their individual trajectories based on solving Newton's equation of motion. Interactions between the particles can include for example hard sphere repulsion, electrostatic repulsion, or Van der Waals attraction. These are added by adding respective forces to the molecular dynamics algorithm.

Dissipative particle dynamics (DPD) on the other hand describes all components of the system in terms of particles on the coarse grained level (as beads representing hundreds or thousands of molecules). In order to compensate for the lost degrees of molecular freedom, drag and noise contributions are added to the equation of motion (which becomes of the Langevin type) and interactions between beads are modeled using purely repulsive soft core potentials. The relative values of these repulsive interaction parameters determine the effective selectivity of beads towards each other. DPD has been used widely for dense fluid systems and complex fluids. Here we show that DPD is also capable of recovering the main features of anisotropic particles on the surface of a liquid bubble (with slightly increased compressibility to imitate air). In order to tackle larger systems of this type, particle methods such as DPD can be coupled to methods based on statistical field theory such as SCFT [24], DDFT [25], or even potentially to Lattice Boltzmann treatments such as the one considered here.

8.1 Lattice-Boltzmann-MD simulations

We performed simulations for different values of the droplet size while keeping the same ellipsoidal particle size. Below we present some snapshots from two simulations performed for two different values of the droplet of the ratio of the droplet diameter to the size of the simulation box Q (Q=0.4 and 0.8). In every simulation we initialized the system by setting the ellipsoidal particles at the fluid-fluid interface while aligning them in the same direction. The number of particles used in the two simulations is different, since putting a large number of particles for smaller droplets can induce numerical instability. This is due to the initial configuration we are using at the moment.

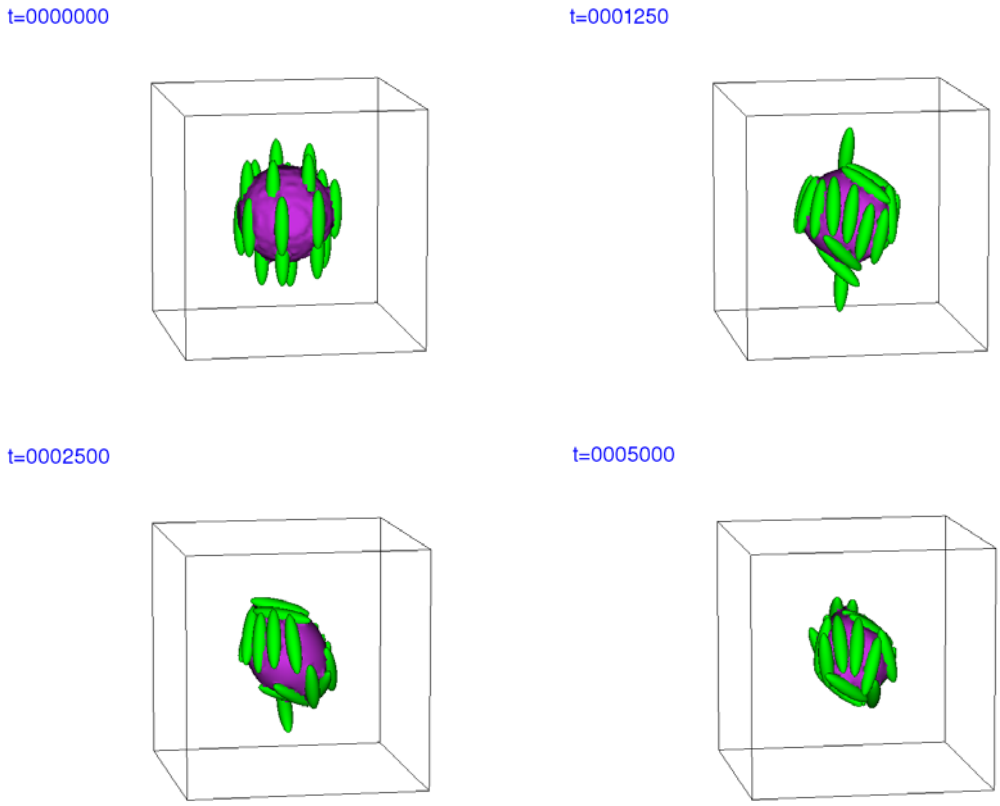

Figure 11. Snapshots taken at different time showing evolution of the reorganization and reorientation of ellipsoidal particles at the interface of a droplet. The smaller droplet case, Q=0.4 (Lattice-Boltzmann simulation)

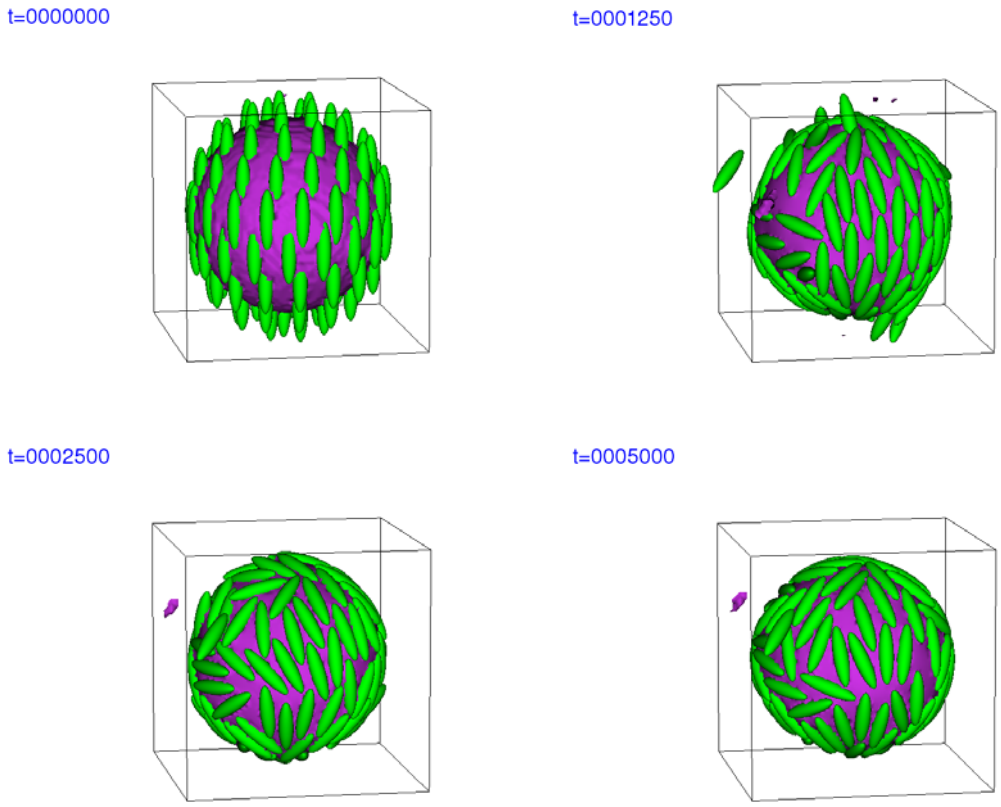

Figure 12. Snapshots showing the evolution in time of the reorganization and the reorientation of ellipsoidal particles at the interface of a droplet for the larger droplet case, Q=0.8 (lattice-Boltzmann simulation)

From the figures we see that after the initial time the particles start readapting their position and orientation with the interface of the droplet. For the case of a smaller droplet, we see that some particles are even expelled from the interface at the beginning of the simulation and later they come back to find a place among other particles. The simulation does not reach any kind of steady state. The system is still evolving. For the case of the larger droplet, the interface adsorbed all the particles and they adapt a direction parallel to the tangential on the droplet interface.

8.2 DPD simulations

Simulations using dissipative particle dynamics were also performed for different droplet sizes and for a number of different rod lengths. In Fig.13 we present selected snapshots from a series of simulations for two selected cases, where the aspect ratio between rod length and droplet diameter was large (of the order of 3.0) and relatively small (around 0.3), keeping the average rod length fixed. Differently than in the previous section, here we initially placed the rods randomly throughout the simulation box and allowed them to assemble at the water—droplet interface, a starting point meant to replicate the experimental non-equilibrium distribution of rods around bubbles after shearing. In all cases the rods associated with the interface (when appropriate interaction parameters were set), inducing the formation of ordered and closely packed domains. The number of rods introduced into the system was estimated based on optimal surface coverage, and the bubble was pinned in the center of the simulation with an attractive external potential.

The character of the domains, and behavior of the rods, is obviously largely controlled by their interactions with the other components, and in the case of DPD simulations, by the

respective interaction parameters. For the largest aspect ratio presented, the rods are longer than the diameter of the droplet, and strongly associate with each other. In this case, the rods formed a nest-like structure with several large, ordered domains that protrude into the bulk phase. For larger droplet sizes, this leads to densly packed multiple layers of rods on the interface.

For the smaller aspect ratio, we present a snapshot where the short-ranged repulsive interactions between rods are more pronounced than in the previous case. This would correspond to adding additional solvent such as alcohol by Zhou et al. in order to balance the association of rods [27]. Returning to our simulations, in this case the domains are more spread out on the droplet surface, and seem to be ordered over large distances on the spherical surface. In contrast, the original experimental images (see [27]) show only local ordering on patches akin to a random deposition process. At this point it is unclear what the reason is for the long range ordering achieved in these simulations. There are three clear possibilities: exaggerated noise due to the crude coarse graining (each DPD bead has a diameter of about 100nm), the still unrealistic shape of the rods, and the monodisperse distribution of rod lengths (as opposed to a highly polydisperse sample originally studied experimentally).

It was within the limits of the workshop to probe the effect of polydispersity, and Fig. 13c shows representative snapshots of an identical simulation to Fig. 13b, but with a polydisperse rod population (same average). Visibly the orientation of rods on the surface appears to be less ordered, and the correlation of rod directions as a function of distance on the surface confirms this (not shown). In order to produce more conclusive results and address the other possibilities, simulations for larger systems need to be performed.

8.3 Conclusions and recommendations

In our simulations we have reproduced the general behavior of rods on a droplet/bubble surface with two different methods, also using different initial conditions. It seems beneficial to try to further bring these different types of simulations closer in terms of system parameters, and to scale them up in size. Although the aspect ratios used are still rough compared to the original problem system, these simulations are a good starting point to address the influence of population polydispersity, shear effects, and other factors.

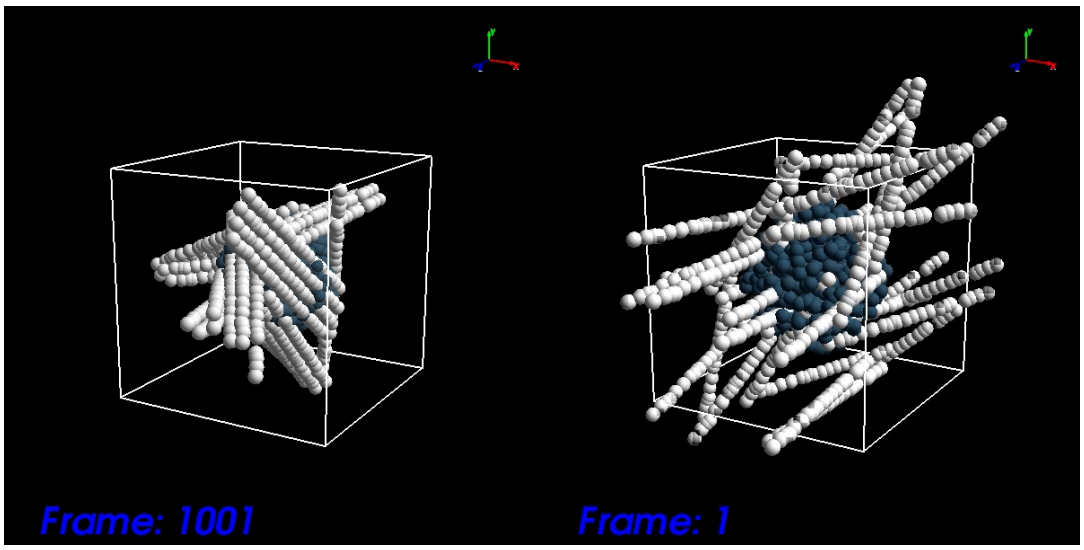

Fig. 13a

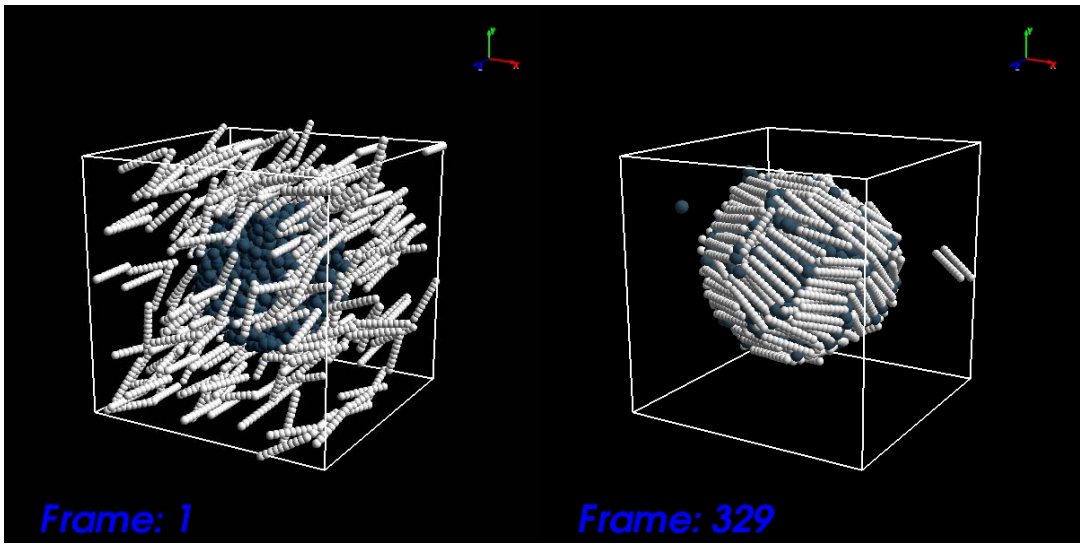

Fig. 13b

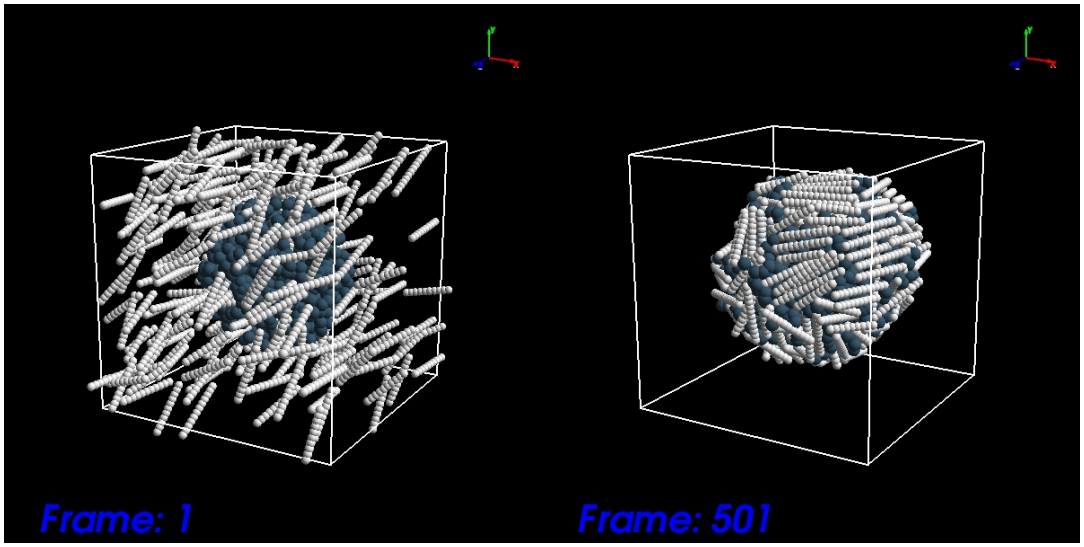

Fig. 13c

Figure 13. Snapshots showing the initial and later stages of selected DPD simulations of rigid rods (modeled as colloids) on bubbles of two sizes. The first simulation (a) is for a bubble with diameter smaller than the rod length, which leads to a nest-like structure. In the other simulations (b and c) the bubble diameter was larger than the length or rods, which in turn were generated from a monodisperse (b) or polydisperse (c) population.

9. Discussion

We have presented the results of our different approaches to the problem of self-assembly on curved surfaces. What we found, firstly, is that although some elements are present in the literature, a lot more research is needed.

We have taken the first steps by looking at the analytical behaviour of the defects and the general geometry of such surfaces. In order to make the analytical calculation more realistic, one might want to add a directional energy cost for domains that fit together but have a different orientation of the rods. Furthermore, a better understanding of the exact energy cost associated with different boundaries is needed.

Our experiments show that the key features of the microscopic self-assembly, such as the formation of domains, can be captured by macroscopic systems. This suggests that the main effects are geometric in nature. Our experiments we limited by the behaviour of the rods at the surface. In the microscopic case, the rods can deform the surface of the bubble and they hardly overlap. We could not reproduce this in our macroscopic systems. As a next step it would be useful to repeat the experiments with a material that can be deformed by the rods and where the rods have more buoyancy.

Finally, the simulations we performed were quite successful in reproducing the general behaviour of the self-assembly, but it seems that the domains that are formed are somewhat larger than in reality. To make these simulations more realistic, one would have to change the aspect ratio of the rods, as well as the size of the bubble and the entire system (easily within reach with these methods). It would be useful to further pursue the question of polydispersity in the rod population along, as demonstrated here for DPD simulations. Although more realistic simulations would be computationally more expensive, it is still possible to do them in a reasonable amount of time within our current framework.

Thus, even though this is only preliminary research, we see some promising results.

10. References

[1] L. Onsager, Ann. (N.Y) Acad. Sci. **51**, 627, 1949.

[2] D. Frenkel and B.M. Mulder, Mol. Phys. **55**, 1171, 1985.

[3] P.G. Bolhuis and D. Frenkel, J. Chem. Phys. **106**, 666, 1997.

[4] M.A. Bates and D. Frenkel, J. Chem. Phys, 112, 22, 2000.

[5] M.A. Bates and Daan Frenkel, J. Chem Phys, 110, 13, 1999.

[6] J.J. Thomson, Philos. Mag. **7**, 237, 1904.

[7] Rainer Backofen et al, Phys Rev. E 81, 025701, 2010.

[8] K Yaman et al, Phys. Rev. Lett 73, 28, 1997.

[9] J. Dzubiella et al, Phys. Rev. E 62, 4, 2000.

[10] M.J. Bowick, Luca Giomi, Adv. in physics, 58, 5, 449-563, 2009.

[11] A.R. Bausch et al, Scinece 299, 5613, pp: 1716-1718, 2003.

[12] T. Lopez-Leon et al, Nature Physics, 7, 391, 2011.

[13] W.T.M. Irvine et al, Nature Letter 468, 947, 2010.

[14] P. Lipowisky et al, Nature Materials 4, 407-411, 2005.

[15] T.C. Lubensky and J. Prost, J. Phys. II France 2, 371, 1992.

[16] D.R. Nelson, Nanoletters 2, 10 p.1125-1129, 2002.

[17] V. Vitelli and D.R. Nelson, Phys. Rev. E 74, 021711, 2006.

[18] T. Lopez-Leon, V. Koning, K.B.S. Devaiah, V. Vitelli, A. Fernadez-Nieves, Nature Physics 7, 391.

[19] P.G. De Gennes and J. Prost (1993), *The Physics of Liquid Crystal Cuboctahedron. (2011, September 10). In Wikipedia, The Free Encyclopedia. Retrieved 07:12, October 25, 2011, from* http://en.wikipedia.org/w/index.php?title=Cuboctahedron&oldid=449573061.

[20] F. David, in *Statistical Mechanics of membranes and surfaces*, D. Nelson, T. Piran, S. Weinberg (2004).

[21] F. Jansen, J. Harting, Phys. Rev. E 83, 046707, 2011.

[22] F. Günther, F. Janoschek, S. Frijters, J. Harting, submitted, arXiv:1109.3277, 2011.

[23] S.W. Sides, B.J. Kim, E.J. Kramer, G.H. Fredrickson, Phys. Rev. Lett. 96, 250601, 2006.

[24] G.J.A. Sevink, and J.G.E.M. Fraaije, *Modelling complex systems in full detail: a new approach*, Complex Systems: 5th International Workshop on Complex Systems, volume 982, 491–496, 2008.

[25] D.M. Hall, T. Lookman, S. Banerjee, Chem. Eng. Sci. 64, 4754–4757, 2009.

[26] W. Zhou, J. Cao, W. Liu, S. Stoyanov, Angew. Chem. Intl. Ed. 49, 378—381, 2009.